Contemporary Mathematics
http://ojs.wiserpub.com/index.php/CM/

Research Article

Solution of the Space Fractional Diffusion Equation Using Quadratic B-Splines and Collocation on Finite Elements

R. A. Adetona, N. Parumasur*, P. Singh

University of KwaZulu-Natal, School of Mathematics Statistics and Computer Science, Private Bag, X54001, Durban 4000, South Africa
E-mail: parumasurn1@ukzn.ac.za

Received: 20 November 2023; **Revised:** 2 January 2024; **Accepted:** 29 January 2024

Abstract: In this paper, we consider the solution of the space fractional diffusion equation using orthogonal collocation on finite elements (OCFE) with quadratic B-spline basis functions. The main advantage of quadratic B-splines is that they have good interpolating properties and can be easily adapted for solving problems on non-uniform grids. The method is unconditionally stable and its convergence is also discussed. It is of order $(3 - \alpha)$ for $1 < \alpha < 2$. We present various linear and nonlinear examples. The solutions compared favourably with previous results in the literature.

***Keywords*:** B-Splines, space fractional diffusion equation, orthogonal collocation, finite elements

MSC: 65L10, 65L60, 65M60, 65M70, 65N35, 35R11

1. Introduction

Fractional differential equations are extension of integer order ordinary and partial differential equations to that of a fractional order. This can be fractional ordinary differential equation (FODE) which involve an independent variable or fractional partial differential equations (FPDE) that consists of several independent variables. Many real life phenomena have been modelled by fractional differential equations. It has applications in long range spatial interactions, anomalous diffusion [1], finance, turbulent flow, physics, chemical kinetics, biology and so on.

The fact that many fractional PDEs do not possess exact solutions has led to proposition of various of numerical methods to solve FPDEs. A finite difference method based on implicit Euler method was used to solve the fractional advection-dispersion flow equation in [2]. Weighted and shifted Grunwald difference operators were used to obtain the numerical solution of the space fractional diffusion equation in [3]. Discrete Galerkin finite element method was used for solving time-fractional diffusion equations in [4]. The fractional derivative considered were in the Caputo sense and the method was found to be of order $(2 - \alpha)$ where $\alpha \in (0, 1)$. Spectral method and finite volume methods for fractional partial differential equations were discussed in [5] and [6] respectively.

The authors of [1] discussed the stability and convergence of quadratic spline collocation method for time-fractional diffusion equation. A combination of method of lines and spline approximation were used to obtain the numerical solution of space fractional diffusion equation by [7]. A cubic B-spline collocation method was employed to solve time fractional wave equation in [8] and anomalous fractional diffusion equation in [9]. A modified spline

DOI: https://doi.org/10.37256/cm.5220243900

collocation was proposed and studied by [10] for linear fractional differential equations.

A time fractional anisotropic diffusion model and numerical schemes for the model were proposed to improve the quality of medical ultrasound images in [11] via meshless method and semi-implicit time integration. A combination of the meshless and Galerkin methods were applied in [12] to two-dimensional time-fractional Tricomi type equations. Collocation coupled with the meshless method was employed by [13] and [14] to solve problems on modified anomalous diffusion and reaction-diffusion processes as two-dimensional fractional differential equations. A kernel based collocation method with greedy algorithm was used to investigate anomalous mobile-immobile solute transport models in [15] as fractional differential equations. In [16], a generalized anomalous mobile-immobile solute transport model with variable coefficients was studied using the meshless technique.

In this paper, we demonstrate the capability of orthogonal collocation using quadratic B-spline basis functions to solve space fractional diffusion equation effectively. The main advantage of quadratic B-splines is that they have good interpolating properties and can be easily adapted for solving problems on non-uniform grids. The method is unconditionally stable and its convergence is also discussed. It is of order $(3 - \alpha)$ for $1 < \alpha < 2$.

The paper is arranged as follows: section 1 is for introduction, section 2 discuss the derivation of fractional B-spline derivative and in section 3, we applied the method to the space fractional diffusion equation. Section 4 deals with the stability of OCFE while section 5 deals with convergence analysis. Numerical examples are provided in section 6 and section 7 concludes the paper.

2. Derivation of fractional B-spline derivative

Let a fractional partial differential equation

$$\frac{\partial^{\alpha} u(x, t)}{\partial x^{\alpha}} = f(x), 1 < \alpha < 2, \tag{1}$$

with boundary conditions

$$u(a, t) = \delta_1, \ u(b, t) = \delta_2, \tag{2}$$

be given. For t fixed, we may treat equation (1) as an ordinary differential equation. The interval $[a, b]$ is divided into N subintervals $[x_i, x_{i+1}]$, $i = 1, 2, \ldots, N$, called elements. The approximate solution $u_c(x)$ in a subinterval $[x_i, x_{i+1}]$ can be written as

$$u^i(x) \approx u_c^i(x) = \sum_{k=1}^{3} b_k^i B_k(x), \tag{3}$$

where $B_k(x)$ is a quadratic spline basis function defined by

$$B_{i+1}(x) = \binom{j}{i} x^i (1-x)^{j-i}, \ i = 0, 1, 2, \ j = 2. \tag{4}$$

We then apply continuity at internal boundaries such that

$$u_c^{i+1}(x_{i+1}) = u_c^i(x_{i+1}), \ \left.\frac{du_c^{i+1}}{dx}\right|_{x_{i+1}} = \left.\frac{du_c^i}{dx}\right|_{x_{i+1}}. \tag{5}$$

We transform the interval $[x_i, x_{i+1}]$ to [0, 1] via $z = \frac{x - x_i}{h}$ where h is the uniform interval spacing. This gives

$$u_c^{i+1}(0) = u_c^i(1), \quad \left.\frac{du_c^{i+1}}{dz}\right|_{z=0} = \left.\frac{du_c^i}{dz}\right|_{z=1}, \quad i = 1, 2, \ldots, N-1. \tag{6}$$

Then

$$b_1^{i+1} = b_3^i, \quad b_2^{i+1} = 2b_3^i - b_2^i, \quad i = 1 \ldots N-1. \tag{7}$$

Using the first condition in (7), the solution $u(x)$ in (3) can be simplified to

$$u_c(z) = \sum_{k=1}^{3} b_{k+2(i-1)} B_k(z). \tag{8}$$

The boundary conditions in (2) become

$$b_1 = \delta_1, \, b_{2N+1} = \delta_2. \tag{9}$$

We shall make use of the Caputo fractional derivative together with the quadratic B-spline basis functions in (4) to solve equation (1). The Caputo derivative [17] is defined as

$$\frac{\partial^\alpha u(x,t)}{\partial x^\alpha} = \frac{1}{\Gamma(n-\alpha)} \int_a^x \frac{\partial^n u(\xi,t)}{\partial \xi^n} (x-\xi)^{n-1-\alpha} \, d\xi, \quad n-1 < \alpha < n, \tag{10}$$

where $\alpha \in \mathbb{R}$ and $n \in \mathbb{N}$. In our case, we are dealing with diffusion equation, so $n = 2$. Equation (10) is now

$$\frac{\partial^\alpha u(x,t)}{\partial x^\alpha} = \frac{1}{\Gamma(2-\alpha)} \int_a^x \frac{\partial^2 u(\xi,t)}{\partial \xi^2} (x-\xi)^{1-\alpha} \, d\xi, \quad 1 < \alpha < 2. \tag{11}$$

We re-write equation (8) as

$$u_c(x,t) = \sum_{k=1}^{3} b_{k+2(i-1)}(t) B_k(x) \tag{12}$$

to include time dependence for a PDE. Substituting (12) into (11) yields

$$\frac{\partial^\alpha u_c(x,t)}{\partial z^\alpha} = \frac{1}{h^2 \Gamma(2-\alpha)} \sum_{i=1}^{j} \left[\int_{x_i}^{x_{i+1}} \sum_{k=1}^{3} b_{k+2(i-1)}(t) B_k''(\xi) (x-\xi)^{1-\alpha} \, d\xi \right]. \tag{13}$$

We then evaluate (13) at the collocation point $z = 0.5$ to get

$$\left.\frac{\partial^\alpha u^n}{\partial x^\alpha}\right|_{x_{m+\frac{h}{2}}} = \frac{1}{\Gamma(2-\alpha)}\int_{x_1}^{x_{m+\frac{h}{2}}} \frac{(u^n)''(\xi)}{(x_{m+\frac{h}{2}}-\xi)^{\alpha-1}}\,d\xi,$$

$$= \frac{1}{\Gamma(2-\alpha)}\left[\sum_{k=1}^{m-1}\int_{x_k}^{x_{k+1}} \frac{(u^n)''(\xi)}{(x_{m+\frac{h}{2}}-\xi)^{\alpha-1}}\,d\xi + \int_{x_m}^{x_{m+\frac{h}{2}}} \frac{(u^n)''(\xi)}{(x_{m+\frac{h}{2}}-\xi)^{\alpha-1}}\,d\xi\right],$$

$$= \frac{2^{\alpha-1}}{h^\alpha\Gamma(3-\alpha)}\left[\sum_{i=1}^{j}(b_{2k-1}-2b_{2k}+b_{2k+1})\left[(2m-2k+1)^\beta-(2m-2k-1)^\beta\right]\right.$$

$$\left.+b_{2m-1}-2b_{2m}+b_{2m+1}\right]. \tag{14}$$

$$\frac{\partial^\alpha u_c(0.5,t)}{\partial z^\alpha} = \sum_{k=1}^{m} C_\alpha(b_{2k-1}-2b_{2k}+b_{2k+1})\left[(2m+1-2k)^\beta-(2m-1-2k)^\beta\right],$$

$$= C_\alpha \sum_{k=1}^{2N+1} a_{jk}b_k,\ m=1,\ 2,\ \ldots,\ N. \tag{15}$$

where $\beta = 2 - \alpha$, a_{jk} is the coefficient of b_k and $C_\alpha = \dfrac{2^{\alpha-1}}{h^\alpha\Gamma(3-\alpha)}$.

We then incorporate equation (15) into (1) with $x = x_j + 0.5h$ substituted into the right hand side to get N equations. These equations together with the continuity equations and boundary conditions give a square linear system of size ($2N$ + 1) given by

$$C_\alpha P\mathbf{b} = \mathbf{f}, \tag{16}$$

where $\mathbf{b} = [b_1, b_2, \ldots, b_{2N+1}]^T$, $\mathbf{f} = [f_1, f_2, \ldots, f_N, 0, \ldots, 0, a\delta_1, a\delta_2]^T$ and

$$P = \begin{pmatrix}
1 & -2 & 1 & 0 & 0 & \cdots & \cdots & 0 & 0\\
3^\beta-1 & -2(3^\beta-1) & 3^\beta & -2 & 1 & \cdots & \cdots & 0 & 0\\
5^\beta-3^\beta & -2(5^\beta-3^\beta) & 5^\beta-1 & -2(3^\beta-1) & 3^\beta & \cdots & \cdots & 0 & 0\\
\vdots & \vdots & \vdots & \vdots & \vdots & \vdots & \vdots & \vdots & \vdots\\
\cdots & \cdots & \cdots & \cdots & \cdots & \cdots & \cdots & -2 & 1\\
0 & a & -2a & a & 0 & \cdots & \cdots & 0 & 0\\
0 & 0 & 0 & a & -2a & \cdots & \cdots & 0 & 0\\
\vdots & \vdots & \vdots & \vdots & \vdots & \vdots & \vdots & \vdots & \vdots\\
0 & 0 & 0 & 0 & 0 & \cdots & \cdots & a & 0\\
a & 0 & 0 & 0 & 0 & \cdots & \cdots & 0 & 0\\
0 & 0 & 0 & 0 & 0 & \cdots & \cdots & 0 & a
\end{pmatrix}. \tag{17}$$

The solution to the fractional differential equation (1) is then obtained via equation (12). The rate of convergence is calculated as $\log_2 \frac{\| \mathbf{e} \|_\infty^h}{\| \mathbf{e} \|_\infty^{h/2}}$ where the components of **e** are given by $e_i = u_i(x) - U_i(x)$, $u_i(x)$ and $U_i(x)$ are exact and approximate solution at the nodes respectively.

3. Application to fractional diffusion equation

We apply the trapezoid rule to the fractional diffusion equation

$$\frac{\partial u}{\partial t} = \frac{\partial^\alpha u(x, t)}{\partial x^\alpha} + f(x) \tag{18}$$

to get

$$u_i^{j+1} - \frac{\Delta t}{2} D_\alpha u_i^{j+1} = u_i^j + \frac{\Delta t}{2}\left(D_\alpha u_i^j + f_i^{j+1} + f_i^j \right), \tag{19}$$

where j is the index for discrete time t, i is index for discrete x, $Nt = (t_f - t_0)/\Delta t$ is the number of time steps, t_f is the final time, t_0 is the initial time and $D_\alpha u = \frac{\partial^\alpha u(x, t)}{\partial x^\alpha}$. Hence the system can be represented in the form

$$C_\alpha Q \mathbf{b} = \mathbf{R}, \tag{20}$$

where Q is a $(2N + 1)$ square matrix, $\mathbf{b} = [b_1, b_2, \ldots, b_{2N+1}]^T$ and $\mathbf{R} = [R_1, R_2, \ldots, R_N, 0, \ldots, 0, a\delta_1, a\delta_2]^T$.

4. Stability

Consider now the fractional diffusion equation given by

$$u_t - d(x, t) \frac{\partial^\alpha}{\partial x^\alpha} u(x, t) = p(x, t), \tag{21}$$

where $d(x, t)$ and $p(x, t)$ are coefficient of the fractional derivative and the source term respectively. Consider the homogeneous case of (21) i.e $p(x, t) = 0$ and assume that $d(x, t) = d$ is constant.

Apply Crank Nicolson to (21) on $[t_n, t_{n+1}]$ to get

$$\int_{t_n}^{t_{n+1}} u_t dt = d \int_{t_n}^{t_{n+1}} \frac{\partial^\alpha}{\partial x^\alpha} u(x, t) dt, \tag{22}$$

$$u^{n+1} - u^n = d \frac{\Delta t}{2} \left[\frac{\partial^\alpha}{\partial x^\alpha} u^n(x) + \frac{\partial^\alpha}{\partial x^\alpha} u^{n+1}(x) \right], \tag{23}$$

$$u^{n+1} - d\,\frac{\Delta t}{2}\frac{\partial^{\alpha}}{\partial x^{\alpha}}u^{n+1} = u^{n} + d\,\frac{\Delta t}{2}\frac{\partial^{\alpha}}{\partial x^{\alpha}}u^{n}. \tag{24}$$

In the m^{th} interval,

$$u^{n}(x_m) = \sum_{k=1}^{3} b^{n}_{k+2(m-1)} B_k(x_m), \tag{25}$$

$$\frac{\partial^{\alpha}}{\partial x^{\alpha}}u^{n}(x_m) = \sum_{k=1}^{3} b^{n}_{k+2(m-1)}\frac{\partial^{\alpha}}{\partial x^{\alpha}}B_k(x_m), \tag{26}$$

where the superscript n on the coefficients b refer to its values at t_n. Substitute the collocation point $x_m + h/2$ into (24), let $u^{n}_{1/2} = u(x_m + h/2)$, and by using (25) it can be shown that

$$\frac{\partial^{\alpha}}{\partial x^{\alpha}}u^{n}_{\frac{1}{2}} = \frac{2^{\alpha-1}}{h^{\alpha}\Gamma(3-\alpha)} \times \sum_{k=1}^{m-1}\left[(2m-2k+1)^{2-\alpha} - (2m-2k-1)^{2-\alpha} + 1\right]\left(b^{n}_{2m-1} - 2b^{n}_{2m} + b^{n}_{2m+1}\right),$$

$$= C\left(b^{n}_{2m-1} - 2b^{n}_{2m} + b^{n}_{2m+1}\right), \text{ where } C > 0. \tag{27}$$

Equation (24) simplifies to

$$\frac{1}{4}(b^{n+1}_{2m-1} + 2b^{n+1}_{2m} + b^{n+1}_{2m+1}) - \frac{d\Delta tC}{2}(b^{n+1}_{2m-1} - 2b^{n+1}_{2m} + b^{n+1}_{2m+1})$$

$$= \frac{1}{4}(b^{n}_{2m-1} + 2b^{n}_{2m} + b^{n}_{2m+1}) + \frac{d\Delta tC}{2}(b^{n}_{2m-1} - 2b^{n}_{2m} + b^{n}_{2m+1}), \tag{28}$$

$\Rightarrow$

$$b^{n+1}_{2m-1} + 2b^{n+1}_{2m} + b^{n+1}_{2m+1} - 2d\Delta tC(b^{n+1}_{2m-1} - 2b^{n+1}_{2m} + b^{n+1}_{2m+1})$$

$$= b^{n}_{2m-1} + 2b^{n}_{2m} + b^{n}_{2m+1} + 2d\Delta tC(b^{n}_{2m-1} - 2b^{n}_{2m} + b^{n}_{2m+1}). \tag{29}$$

Let $\alpha_1 = 1 - 2\Delta tCd$, $\sigma_1 = 1 + 2\Delta tCd$, $\alpha_2 = 2 + 4\Delta tCd = 2\sigma_1$ and $\sigma_2 = 2 - 4\Delta tCd = 2\alpha_1$. Equation 29 yields

$$\alpha_1 b^{n+1}_{2m-1} + \alpha_2 b^{n+1}_{2m} + \alpha_1 b^{n+1}_{2m+1} = \sigma_1 b^{n}_{2m-1} + \sigma_2 b^{n}_{2m} + \sigma_1 b^{n}_{2m+1}. \tag{30}$$

Let $b^{n}_{l} = \lambda^{n} e^{ilhk}$, $i = \sqrt{-1}$, k is mode, we have

$$\alpha_1\lambda^{n+1}e^{i(2m-1)hk}+\alpha_2\lambda^{n+1}e^{i2mhk}+\alpha_1\lambda^{n+1}e^{i(2m+1)hk}$$

$$=\sigma_1\lambda^{n}e^{i(2m-1)hk}+\sigma_1\lambda^{n}e^{i2mhk}+\sigma_1\lambda^{n}e^{i(2m+1)hk}. \tag{31}$$

Therefore

$$\frac{\lambda^{n+1}}{\lambda^{n}}=\frac{\sigma_1\left(e^{-ihk}+e^{ihk}\right)+\sigma_2}{\alpha_1\left(e^{-ihk}+e^{ihk}\right)+\alpha_2},$$

$$=\frac{\alpha_2\cos(hk)+\sigma_2}{2\alpha_1\cos(hk)+\alpha_2}, \tag{32}$$

$$\lambda=\frac{\alpha_2\cos(hk)+4-\alpha_2}{(4-\alpha_2)\cos(hk)+\alpha_2}.$$

$$|\lambda|^2=\frac{\alpha_2^2\cos^2(hk)+2\alpha_2(4-\alpha_2)\cos(hk)+(4-\alpha_2)^2}{(4-\alpha_2)^2\cos^2(hk)+2\alpha_2(4-\alpha_2)\cos(hk)+\alpha_2^2}=\frac{N}{D}.$$

$$N-D=\left((4-\alpha_2)^2-\alpha_2^2\right)-\left((4-\alpha_2)^2-\alpha_2^2\right)\cos^2(hk),$$

$$=\left((4-\alpha_2)^2-\alpha_2^2\right)\sin^2(hk),$$

$$=4(4-2\alpha_2)\sin^2(hk),$$

$$=8(2-\alpha_2)\sin^2(hk),$$

$$=-32\Delta tCd\sin^2(hk)\le 0,\ \text{for } d>0. \tag{33}$$

$\Rightarrow N\le D\Rightarrow|\lambda|\le 1$. Hence our method is unconditionally stable.

5. Convergence analysis

Having shown that our method is stable in the previous section, we now show that our method is consistent. The determinant of the coefficient matrix $C_\alpha P$ is $\det(C_\alpha P)=(-1)^{[N/2]}2N(C_\alpha)^N\neq 0$ for all values of α. Therefore the coefficient matrix is nonsingular. This implies that our method is consistent. Hence our method is convergent.

We now consider (1) and illustrate the convergence analysis for the fractional partial differential equation for a fixed t. This is equivalent to the fractional ordinary differential equation

$$D^{\alpha}u=\lambda u,$$

where λ is a constant. This simplifies to

$$\int_a^x \frac{u''(s)}{(x-s)^{\alpha-1}} ds = \Gamma(2-\alpha)\lambda u$$

$$= f(x). \tag{34}$$

Let $x_i = x_1 + (i-1)h$, $i = 1, 2, \ldots, N+1$, the collocation points are at

$$\overline{x}_i = x_i + \frac{h}{2} = x_1 + \left(i - \frac{1}{2}\right)h.$$

The collocation solution in the i_{th} interval is

$$u_c^i = \sum_{j=1}^{3} b_{j+2(i-1)} B_j(z),$$

$$= b_{2i-1}B_1(z) + b_{2i}B_2(z) + b_{2i+1}B_3(z),$$

Then

$$u_c^{i''}(x) = \frac{2}{h^2}\left[b_{2i-1} - 2b_{2i} + b_{2i+1}\right].$$

If x is in the i_{th} interval,

$$\int_{x_1}^x \frac{u''(s)}{(x-s)^{\alpha-1}} ds = \sum_{k=1}^{i-1} I_k + I_i \tag{35}$$

with I_k defined as

$$I_k = \int_{x_k}^{x_{k+1}} \frac{u^{(k)''}(s)}{(x-s)^{\alpha-1}} ds,$$

$$= \frac{2}{h^2(2-\alpha)}\left[(x-x_k)^{2-\alpha} - (x-x_{k+1})^{2-\alpha}\right]\left(b_{2k-1} - 2b_{2k} + b_{2k+1}\right),$$

$$k = 1, 2, \ldots, i-1. \tag{36}$$

Therefore

$$I_i(x) = \int_{x_i}^{x} \frac{u^{(i)''}(s)}{(x-s)^{\alpha-1}} ds,$$

$$= \frac{2(x-x_i)^{2-\alpha}}{h^2(2-\alpha)} \left[b_{2i-1} - 2b_{2i} + b_{2i+1} \right]. \tag{37}$$

Substitute the collocation points $\bar{x}_i$, $i = 1, 2, \ldots, N$ into (36) and (37) to get

$$I_k(x_i) = \frac{2^{\alpha-1}}{2-\alpha} h^{-\alpha} \left[(2i-2k+1)^{2-\alpha} - (2i-2k-1)^{2-\alpha} \right],$$

$$\left(b_{2k-1} - 2b_{2k} + b_{2k+1} \right), k < i. \tag{38}$$

$$I_i(x_i) = \frac{2^{\alpha-1}}{2-\alpha} h^{-\alpha} \left[b_{2i-1} - 2b_{2i} + b_{2i+1} \right]. \tag{39}$$

Hence, substitute the collocation points $\bar{x}_i$ into (34) gives

$$c_\alpha \left[\sum_{k=1}^{i-1} \left[(2i-2k+1)^{2-\alpha} - (2i-2k-1)^{2-\alpha} \right] \right.$$

$$\left. \times \left(b_{2k-1} - 2b_{2k} + b_{2k+1} \right) + \left(b_{2i-1} - 2b_{2i} + b_{2i+1} \right) \right] = f(\bar{x}_i), \tag{40}$$

where $c_\alpha = \frac{2^{\alpha-1} h^{-\alpha}}{2-\alpha}$ and $i = 1, 2, \ldots, N$.

We now define a linear operator L by $(Lu)(x) = \int_a^x \frac{u''(s)}{(x-s)^{\alpha-1}} ds$. Let x be in $[x_i, x_{i+1}]$ and $\bar{x}_i$ be the midpoint of $[x_i, x]$ so that the length of this interval is given by $w_i h$ for $w_i \in (0, 1]$. Define $e(x) = u(x) - u_c(x)$

$$Le(x) = \sum_{k=1}^{i-1} \int_{x_k}^{x_{k+1}} \frac{e''(s)}{(x-s)^{\alpha-1}} ds + \int_{x_i}^{x} \frac{e''(s)}{(x-s)^{\alpha-1}} ds, \tag{41}$$

$$= \sum_{k=1}^{i-1} e''(\xi_k) \int_{x_k}^{x_{k+1}} \frac{1}{(x-s)^{\alpha-1}} ds + e''(\xi_i) \int_{x_i}^{x} \frac{1}{(x-s)^{\alpha-1}} ds, \tag{42}$$

where we have used the integral mean value theorem, $\xi_k \in (x_k, x_{k+1})$ and $\xi_i \in (x_i, x)$. Now

$$e''(\xi_k) = u''(\xi_k) - u_c''(\xi_k),$$

$$= u''(\xi_k) - u_c''(\bar{x}_k),$$

since $u_c''(x)$ is constant in $[x_k, x_{k+1}]$.

We assume that for $h << 1$, ξ_k can be approximated by $\bar{x}_k$ so that $e''(\xi_k) = e''(\bar{x}_k) = u''(\bar{x}_k) - u_c''(\bar{x}_k)$. By Taylor's theorem,

$$u(x_{k+1}) = u(\bar{x}_k + \frac{h}{2}) = \sum_{p=0}^{3} \frac{u^{(p)}(\bar{x}_k)}{p!}\left(\frac{h}{2}\right)^p + u^4(\beta_1)\left(\frac{h}{2}\right)^4, \ \beta_1 \in (\bar{x}_k, x_{k+1}).$$

$$u(x_k) = u(\bar{x}_k - \frac{h}{2}) = \sum_{p=0}^{3} (-1)^p \frac{u^{(p)}(\bar{x}_k)}{p!}\left(\frac{h}{2}\right)^p + u^4(\beta_2)\left(\frac{h}{2}\right)^4, \ \beta_2 \in (x_{k-1}, \bar{x}_k).$$

Thus $u(x_{k+1}) + u(x_k) = 2u(\bar{x}_k) + u''(\bar{x}_k)\frac{h^2}{2} + O(h^4)$.

$$u''(\bar{x}_k) = \frac{2}{h^2}\left[u(x_{k+1}) - 2u(\bar{x}_k) + u(x_k)\right] + O(h^2), \tag{43}$$

$$u_c''(\bar{x}_k) = \frac{2}{h^2}\left[b_{2k-1} - b_{2k} + b_{2k+1}\right]. \tag{44}$$

Now $b_{2k-1} = u_c(x_k)$ and $b_{2k+1} = u_c(x_{2k+1})$,

$$u_c(\bar{x}_k) = \frac{1}{4}\left(b_{2k-1} + b_{2k+1}\right) + \frac{1}{2}b_{2k},$$

$$= \frac{1}{2}\left(\frac{u_c(x_k) + u_c(x_{k+1})}{2}\right) + \frac{1}{2}b_{2k},$$

$$\approx \frac{1}{2}u_c(\bar{x}_k) + \frac{1}{2}b_{2k}. \tag{45}$$

We have assumed that the collocation solution at the midpoint of $[x_k, x_{k+1}]$ is approximately the average of the solutions at the endpoints. Hence $b_{2k} \approx u_c(\bar{x}_k)$.

$$u_c''(x_k) = \frac{2}{h^2}\left[u_c(x_{k+1}) - 2u_c(\bar{x}_k) + u_c(x_k)\right]. \tag{46}$$

We assume that the approximation of the second derivative in (43) agrees closely with that in (46), thus

$$u''(\bar{x}_k) - u_c(\bar{x}_k) = O(h^2). \tag{47}$$

Hence

$$|e''(s_k)| \leq M_k h^2, \tag{48}$$

for some constant M_k.

Equation (47) has been verified numerically. We shall approximate the integral using the midpoint rule.

$$\int_{x_k}^{x_{k+1}} \frac{1}{(x-s)^{\alpha-1}} ds = \frac{h}{(x-\bar{x}_k)^{\alpha-1}} + g''(\bar{\xi}_k)\frac{h^3}{24}, \tag{49}$$

where $g(s) = \dfrac{1}{(x-s)^{\alpha-1}}$ and $\bar{\xi}_k \in (x_k, x_{k+1})$. Hence

$$\sum_{k=1}^{i-1} \int_{x_k}^{x_{k+1}} \frac{1}{(x-s)^{\alpha-1}} ds = h\sum_{k=1}^{i-1} \frac{1}{(x-\bar{x}_k)^{\alpha-1}} + \frac{h^3}{24}\sum_{k=1}^{i-1} g''(\bar{\xi}_k),$$

$$\leq \frac{h(i-1)}{(x-\bar{x}_i)^{\alpha-1}} + \frac{\alpha(\alpha-1)h^3}{24}\sum_{k=1}^{i-1}\frac{1}{(x-\bar{\xi}_k)^{\alpha+1}},$$

$$\leq \frac{h(i-1)}{(x-x_i)^{\alpha-1}} + \frac{\alpha(\alpha-1)h^3}{24}(i-1)\frac{1}{(x-x_i)^{\alpha+1}}. \tag{50}$$

Similarly, the second term in (41) can be simplified to

$$\int_{x_i}^{x} \frac{e''(s)}{(x-s)^{\alpha-1}} ds \leq M_i h^2 \left[\frac{w_1 h}{(x-\bar{x}_i)^{\alpha-1}} + g''(\bar{\xi}_i)\frac{w_1^3 h^3}{24}\right], \quad \bar{\xi}_i \in (x_i, x),$$

$$\leq M_i h^2 \left[\frac{w_1 h}{(x-\bar{x}_i)^{\alpha-1}} + \frac{\alpha(\alpha-1)w_1^3 h^3}{24}\frac{1}{(x-\bar{\xi}_i)^{\alpha+1}}\right]. \tag{51}$$

If $\bar{x}_i = x_i + w_2 h$, $\bar{\xi}_i = x_i + w_3 h$, $w_2, w_3 \in (0, 1)$ and $M_i = \max_{k \leq i-1} M_k$ then from (42), (48), (50) and (51) it follows that

$$|Le(x)| \leq M_1 h^3 (i-1)\left[\frac{1}{(x-x_i)^{\alpha-1}} + \frac{\alpha(\alpha-1)h^2}{24}\frac{1}{(x-x_i)^{\alpha+1}}\right]$$

$$+M_i h^3 \left[\frac{w_1}{(x-x_i-w_2 h)^{\alpha-1}} + \frac{\alpha(\alpha-1)}{24}\frac{w_1^3 h^2}{(x-x_i-w_3 h)^{\alpha+1}}\right]. \tag{52}$$

The function on the RHS of (52) is an upper bound for $|Le(x)|$ $\forall x$. In particular, when $x = x_{N+1}$, $i = N$, we have

$$|| L\, e(x) ||_\infty = M_1 h^{4-\alpha}(N-1)\left[1+\frac{\alpha(\alpha-1)}{24}\right]$$

$$+M_N h^{4-\alpha}\left[\frac{w_1}{1-w_2}+\frac{\alpha(\alpha-1)}{24}\frac{w_1^3}{1-w_3}\right]. \tag{53}$$

But $N-1 \approx N \propto h^{-1}$ for large N. Thus there exists constants k_1 and k_2 such that

$$\left\|L\, e(x)\right\|_\infty \le k_1 h^{3-\alpha} + k_2 h^{4-\alpha}. \tag{54}$$

Now assuming that L^{-1} is bounded above, we have

$$\begin{aligned}\left|(u-u_c)(x)\right| &\le \left\|(u-u_c)(x)\right\|_\infty,\\ &= \left\|L^{-1}L(u-u_c)(x)\right\|_\infty,\\ &\le \left\|L^{-1}\right\|\left\|L\, e(x)\right\|_\infty,\\ &= O(h^{3-\alpha}),\end{aligned} \tag{55}$$

from (54). This shows that the fractional partial differential equation (1) is of order $(3-\alpha)$ in space.

We then infer from the trapezoid rule that the local error is given by $\frac{\Delta t^3}{12}u_{tt}(x, \xi_n)$, $\xi_n \in [t_n, t_{n+1}]$. Let $u(x, t_{n+1})$ be the exact solution of (1), and assume that $u(x, t_{n+1}) \in C^4[a, b]$. At time t_{n+1}, the global error is $t_{n+1}K\Delta t^2$ for constant K. Hence

$$\begin{aligned}\left\|u_c(x, t_{n+1}) - u(x, t_{n+1})\right\|_\infty &= O(K\Delta t^2 + h^{3-\alpha}),\\ &= O(K\Delta t^2 + \Delta x^{3-\alpha}),\end{aligned} \tag{56}$$

for some constants K.

6. Numerical examples

In this section we illustrate our method with some examples as follows:

6.1 *First example*

We consider the equation

$$\frac{\partial u}{\partial t}-\frac{24x^{\alpha}}{\Gamma(5+\alpha)}\frac{\partial^{\alpha}u}{\partial x^{\alpha}}+2u=0 \tag{57}$$

with initial condition

$$u(x,\,0)=x^{4+\alpha} \tag{58}$$

and boundary conditions

$$\left.\begin{aligned}u(0,\,t)&=0,\\ u(1,\,t)&=e^{-t}.\end{aligned}\right\} \tag{59}$$

The exact solution is $u(x, t)=x^{\alpha+4}e^{-t}$.

The linearized form of (57) is

$$(1+\Delta t)u_i^{j+1}-\frac{\Delta t}{2}m_iD_{\alpha}u_i^{j+1}=(1-\Delta t)u_i^{j}+\frac{\Delta t}{2}m_iD_{\alpha}u_i^{j}, \tag{60}$$

where $m(x)=\dfrac{24x^{\alpha}}{\Gamma(5+\alpha)}$.

Table 1. Comparison of L_{∞} errors when $h=\Delta t$ at $t=1$

h	$\alpha=1.2$		$\alpha=1.4$	
	[18]	Present	[18]	Present
1/15	2.931×10^{-3}	4.756×10^{-4}	2.377×10^{-3}	6.540×10^{-4}
1/20	1.709×10^{-3}	2.875×10^{-4}	1.360×10^{-3}	4.203×10^{-4}
1/25	1.111×10^{-3}	1.938×10^{-4}	8.761×10^{-4}	2.971×10^{-4}
1/30	7.777×10^{-4}	1.401×10^{-4}	6.134×10^{-4}	2.233×10^{-4}

Table 2. Comparison of L_{∞} errors when $h=\Delta t$ at $t=1$

h	$\alpha=1.5$		$\alpha=1.8$	
	[18]	Present	[18]	Present
1/15	2.138×10^{-3}	7.221×10^{-4}	1.445×10^{-3}	5.862×10^{-4}
1/20	1.221×10^{-3}	4.789×10^{-4}	8.284×10^{-4}	4.342×10^{-4}
1/25	7.874×10^{-4}	3.466×10^{-4}	5.369×10^{-4}	3.428×10^{-4}
1/30	5.498×10^{-4}	2.656×10^{-4}	3.763×10^{-4}	2.828×10^{-4}

In Tables 1 and 2, we compared our method with that of [18] for different values of α. It is clear from the tables that our method is better than that of [18].

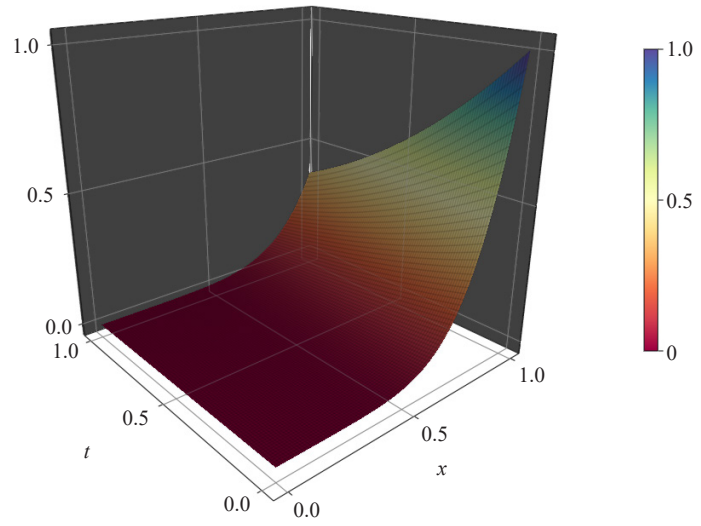

Figure 1. 3D plot of solution at $N = Nt = 50$, $\alpha = 1.5$

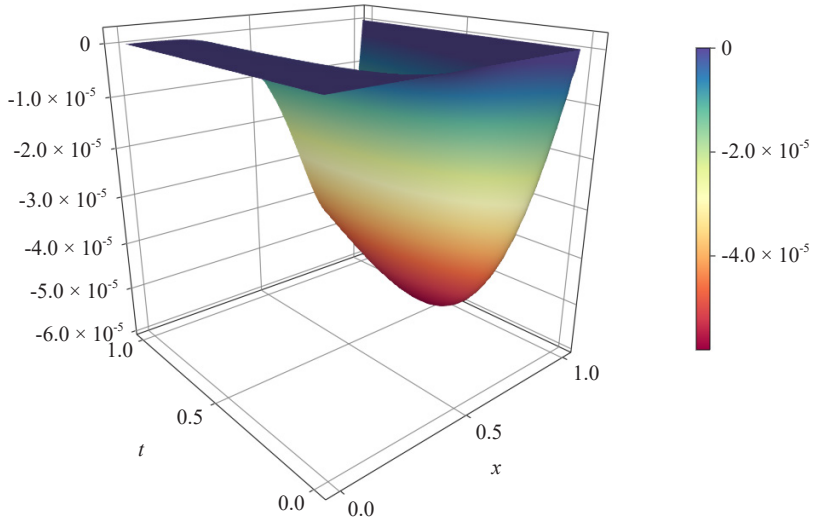

Figure 2. Error plot at $N = Nt = 50$, $\alpha = 1.5$

Table 3 shows that as α is increasing, absolute error is increasing. Table 4 shows that the convergence order is $(3 - \alpha)$. Figures 1 and 2 display the efficiency of quadratic spline to handle fractional diffusion equation using a small number of intervals.

Table 3. Table of absolute errors at for different values of α when $N = Nt = 50$

x	$\alpha = 1.1$	$\alpha = 1.3$	$\alpha = 1.5$	$\alpha = 1.8$
0.10	1.560×10^{-8}	1.590×10^{-8}	1.390×10^{-8}	6.300×10^{-9}
0.30	5.330×10^{-7}	8.570×10^{-7}	1.190×10^{-6}	1.140×10^{-6}
0.50	2.680×10^{-6}	5.380×10^{-6}	9.230×10^{-6}	1.220×10^{-5}
0.70	7.650×10^{-6}	1.760×10^{-5}	3.300×10^{-5}	4.930×10^{-5}
0.90	8.830×10^{-6}	2.030×10^{-5}	3.960×10^{-5}	6.450×10^{-5}
0.98	2.420×10^{-6}	5.820×10^{-6}	1.180×10^{-5}	2.000×10^{-5}

Table 4. Convergence rates for different values of α when $N = Nt = 50$

x	$\alpha = 1.1$	$\alpha = 1.3$	$\alpha = 1.5$	$\alpha = 1.8$
0.10	1.7746	1.5451	1.2872	0.5882
0.30	1.8834	1.6746	1.4615	1.0995
0.50	1.8900	1.6834	1.4760	1.1411
0.70	1.8892	1.6814	1.4768	1.1522
0.90	1.8872	1.6808	1.4771	1.1561
0.98	1.8860	1.6802	1.4771	1.1570
Ord_{∞}	1.8649	1.6599	1.4545	1.1060

6.2 *Second example*

We consider the equation

$$\frac{\partial u}{\partial t} - \frac{\Gamma(5-\alpha)}{24} x^{\alpha} \frac{\partial^{\alpha} u}{\partial x^{\alpha}} + 2u = 0 \tag{61}$$

with initial condition

$$u(x, 0) = x^4 \tag{62}$$

and boundary conditions

$$\left.\begin{aligned} u(0,t) &= 0, \\ u(1,t) &= e^{-t}. \end{aligned}\right\} \tag{63}$$

The exact solution is $u(x, t) = x^4 e^{-t}$.

The linearized form of (61) is

$$(1+\Delta t)u_i^{j+1} - \frac{\Delta t}{2} m_i D_\alpha u_i^{j+1} = (1-\Delta t)u_i^j + \frac{\Delta t}{2} m_i D_\alpha u_i^j, \tag{64}$$

where $m(x) = \dfrac{\Gamma(5-\alpha)}{24} x^\alpha$.

Graphical solution for this problem is similar to that of example 6.1. Hence the graphs are not repeated here. Tables 5 and 6 show the comparison between the present work and that of [18] for different values of α. It is clear that the present results are better than that of [18] due to lower infinity norm of errors.

Table 5. Comparison of L_∞ errors when $h = \Delta t$ at $t = 1$

h	$\alpha = 1.2$		$\alpha = 1.4$	
	[18]	Present	[18]	Present
1/15	1.170×10^{-3}	2.318×10^{-4}	8.679×10^{-4}	3.212×10^{-4}
1/20	7.122×10^{-4}	1.387×10^{-4}	5.162×10^{-4}	2.050×10^{-4}
1/25	4.801×10^{-4}	9.303×10^{-5}	3.401×10^{-4}	1.445×10^{-4}
1/30	3.432×10^{-4}	6.758×10^{-5}	2.411×10^{-4}	1.090×10^{-4}

Table 6. Comparison of L_∞ errors when $h = \Delta t$ at $t = 1$

h	$\alpha = 1.5$		$\alpha = 1.8$	
	[18]	Present	[18]	Present
1/15	7.439×10^{-4}	3.584×10^{-4}	4.361×10^{-4}	3.186×10^{-4}
1/20	4.399×10^{-4}	2.361×10^{-4}	2.532×10^{-4}	2.323×10^{-4}
1/25	2.880×10^{-4}	1.704×10^{-4}	1.645×10^{-4}	1.808×10^{-4}
1/30	2.040×10^{-4}	1.309×10^{-4}	1.158×10^{-4}	1.470×10^{-4}

6.3 *Third example*

We consider the fractional diffusion equation

$$\frac{\partial u}{\partial t} - \Gamma(3-\alpha)\, x^{\alpha-1} \frac{\partial^{\alpha} u}{\partial x^{\alpha}} = (x^2+1)\cos(t+1) - 2x\sin(t+1) \tag{65}$$

with initial condition

$$u(x,\, 0) = (x^2+1)\sin(1) \tag{66}$$

and boundary conditions

$$\left.\begin{aligned} u(0,\, t) &= \sin(t+1), \\ u(1,\, t) &= 2\sin(t+1). \end{aligned}\right\} \tag{67}$$

The exact solution is $u(x, t) = (x^2 + 1)\sin(t + 1)$.

The linearized form of (65) is

$$u_i^{j+1} - \frac{\Delta t}{2} m_i D_{\alpha} u_i^{j+1} = u_i^{j} + \frac{\Delta t}{2} m_i D_{\alpha} u_i^{j} + \frac{\Delta t}{2}(r_i^{j+1} + r_i^{j}), \tag{68}$$

where $m(x) = \Gamma(3 - \alpha)\, x^{\alpha-1}$ and $r(x, t) = (x^2 + 1)\cos(t + 1) - 2x\sin(t + 1)$.

Table 7. Comparison of L_{∞} errors when $h = \Delta t$ at $t = 1$

h	$\alpha = 1.2$		$\alpha = 1.4$	
	[18]	Present	[18]	Present
1/15	1.157×10^{0}	1.992×10^{-5}	3.246×10^{-2}	1.674×10^{-5}
1/20	7.135×10^{-1}	1.102×10^{-5}	1.936×10^{-2}	9.021×10^{-6}
1/25	2.023×10^{0}	6.983×10^{-6}	1.287×10^{-2}	5.607×10^{-6}
1/30	3.747×10^{0}	4.817×10^{-6}	9.106×10^{-3}	3.811×10^{-6}

Table 8. Comparison of L_{∞} errors when $h = \Delta t$ at $t = 1$

h	$\alpha = 1.5$		$\alpha = 1.8$	
	[18]	Present	[18]	Present
1/15	1.729×10^{-2}	1.714×10^{-5}	2.169×10^{-3}	2.159×10^{-5}
1/20	1.097×10^{-2}	9.099×10^{-6}	1.696×10^{-3}	1.169×10^{-5}
1/25	7.729×10^{-3}	5.606×10^{-6}	1.375×10^{-3}	7.261×10^{-6}
1/30	5.878×10^{-3}	3.784×10^{-6}	1.145×10^{-3}	4.924×10^{-6}

We compared the infinity norm of errors for different values of α in Tables 7 and 8. We found that B-spline collocation approximation is better than corresponding finite difference approximation of the same order for the fractional diffusion equation.

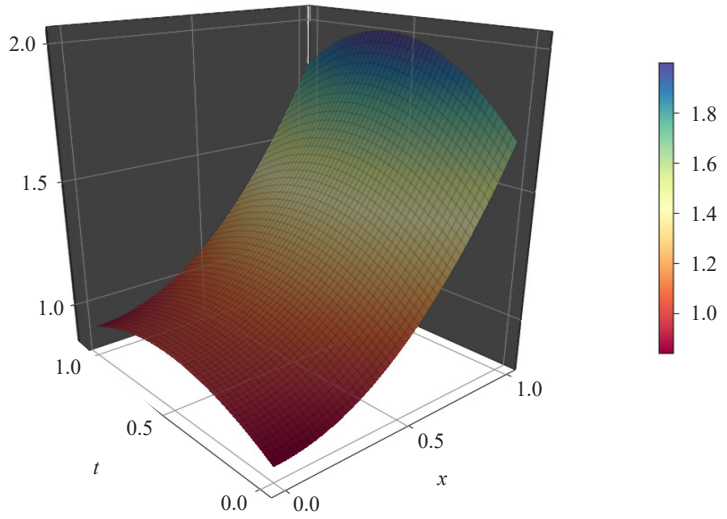

Figure 3. 3D plot of solution at $N = Nt = 50$, $\alpha = 1.5$

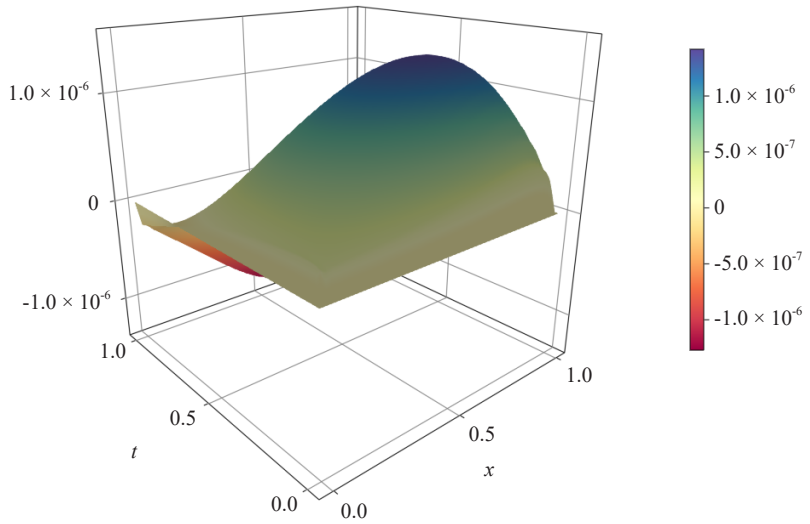

Figure 4. Error plot at $N = Nt = 50$, $\alpha = 1.5$

Table 9 shows that absolute error decreases as α increases except when $\alpha = 1.8$. The convergence order is shown in Table 10. Ord_∞ represents the global order computed using the L_∞ norm. The nodal order is better than the global order. Figure 3 showed the approximate solution overlaid with a mesh plot of the exact solution. There is a perfect match between the exact and approximate solutions. The error is represented by Figure 4.

Table 9. Table of absolute errors at for different values of α when $N = Nt = 50$

x	$\alpha = 1.1$	$\alpha = 1.3$	$\alpha = 1.5$	$\alpha = 1.8$
0.10	9.290×10^{-8}	5.650×10^{-8}	7.730×10^{-8}	2.140×10^{-7}
0.30	3.590×10^{-7}	1.930×10^{-7}	1.790×10^{-7}	3.260×10^{-7}
0.50	5.600×10^{-7}	3.190×10^{-7}	2.720×10^{-7}	3.780×10^{-7}
0.70	5.310×10^{-7}	3.440×10^{-7}	2.890×10^{-7}	3.440×10^{-7}
0.90	2.310×10^{-7}	1.820×10^{-7}	1.530×10^{-7}	1.650×10^{-7}
0.98	5.110×10^{-8}	4.260×10^{-8}	3.590×10^{-8}	3.780×10^{-8}

Table 10. Convergence rates for different values of α when $N = Nt = 50$

x	$\alpha = 1.1$	$\alpha = 1.3$	$\alpha = 1.5$	$\alpha = 1.8$
0.10	2.0591	2.2555	2.3884	2.1976
0.30	2.0094	2.0823	2.2073	2.1587
0.50	2.0047	2.0439	2.1293	2.1302
0.70	2.0084	2.0285	2.0903	2.1096
0.90	2.0066	2.0204	2.0678	2.0948
0.98	2.0039	2.0182	2.0614	2.0925
Ord_{∞}	1.5247	1.5753	1.6783	1.6419

6.4 *Fourth example*

We consider the linear fractional diffusion equation

$$\frac{\partial u}{\partial t} - \Gamma(4-\alpha)\, x^{\alpha}\, \frac{\partial^{\alpha} u}{\partial x^{\alpha}} + 7u = 2\alpha x^2 e^{-t} \tag{69}$$

with initial condition

$$u(x,\, 0) = x^2 - x^3 \tag{70}$$

and boundary conditions

$$\left.\begin{aligned} u_x(0,\, t) &= 0, \\ u_x(1,\, t) &= -8e^{-t}. \end{aligned}\right\} \tag{71}$$

The exact solution is $u(x, t) = (x^2 - x^3)e^{-t}$.

The linearized form of (69) is

$$\left[1+\frac{7\Delta t}{2}\right]u_i^{j+1} - \frac{\Delta t}{2}m_i D_\alpha u_i^{j+1} = \left[1-\frac{7\Delta t}{2}\right]u_i^j + \frac{\Delta t}{2}m_i D_\alpha u_i^j + \frac{\Delta t}{2}(r_i^{j+1} + r_i^j), \tag{72}$$

where $m(x) = \Gamma(4 - \alpha)\, x^\alpha$ and $r(x, t) = 2\alpha x^2 e^{-t}$.

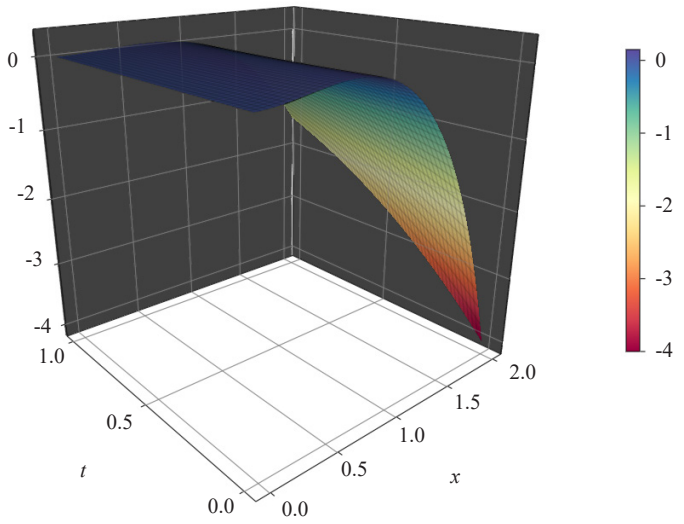

Figure 5. 3D plot of solution at $N = Nt = 50$, $\alpha = 1.5$

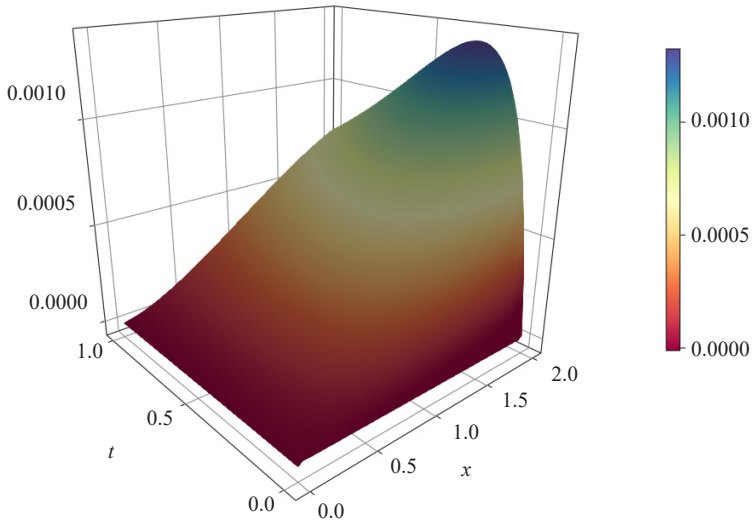

Figure 6. Error plot at $N = Nt = 50$, $\alpha = 1.5$

Figures 5 and 6 show the approximate solution and the error respectively when $\alpha = 1.5$. In Table 11, as α is increasing, the absolute error is increasing. The convergence order in Table 12 is approximately $(3 - \alpha)$. Therefore the

approximate solution shown in for $\alpha = 1.5$ is of higher accuracy than that of $\alpha = 1.8$ but less accurate than that of $\alpha = 1.3$.

Table 11. Table of absolute errors at for different values of α

x	$\alpha = 1.1$	$\alpha = 1.3$	$\alpha = 1.5$	$\alpha = 1.8$
0.20	4.790×10^{-6}	7.910×10^{-6}	1.180×10^{-5}	1.400×10^{-5}
0.60	1.680×10^{-5}	3.270×10^{-5}	5.860×10^{-5}	9.150×10^{-5}
0.80	2.360×10^{-5}	4.700×10^{-5}	8.700×10^{-5}	1.440×10^{-4}
1.00	3.120×10^{-5}	6.190×10^{-5}	1.170×10^{-4}	2.010×10^{-4}
1.20	3.960×10^{-5}	7.720×10^{-5}	1.460×10^{-4}	2.570×10^{-4}
1.40	4.910×10^{-5}	9.260×10^{-5}	1.740×10^{-4}	3.110×10^{-4}
1.96	8.290×10^{-5}	1.350×10^{-4}	2.350×10^{-4}	4.120×10^{-4}

Table 12. Convergence rates for different values of α

x	$\alpha = 1.1$	$\alpha = 1.3$	$\alpha = 1.5$	$\alpha = 1.8$
0.20	1.8995	1.6960	1.4959	1.1996
0.60	1.9066	1.7113	1.5117	1.2143
0.80	1.9118	1.7197	1.5195	1.2218
1.00	1.9180	1.7298	1.5289	1.2307
1.20	1.9249	1.7417	1.5402	1.2415
1.40	1.9323	1.7557	1.5539	1.2547
1.96	1.9542	1.8060	1.6097	1.3129
Ord_{∞}	1.9027	1.7797	1.6103	1.0966

6.5 *Fifth example*

We take a nonlinear fractional partial differential equation

$$\frac{\partial u}{\partial t} - \Gamma(3-\alpha)\, x^{2+\alpha} t\, \frac{\partial^{\alpha} u}{\partial x^{\alpha}} + 2u^2 = x^2 \tag{73}$$

with initial condition

$$u(x, 0) = 0 \tag{74}$$

and boundary conditions

$$\left.\begin{aligned} u(0,t)+u_x(0,t)&=0,\\ u(1,t)+u_x(1,t)&=(2e^{-t}+1)t. \end{aligned}\right\} \tag{75}$$

The exact solution is $u(x, t) = tx^2$.
The linearized form of (73) is

$$(1+2u^j\Delta t)u_i^{j+1}-\frac{\Delta t}{2}m_i^{j+1}D_\alpha u_i^{j+1}=u_i^j+\frac{\Delta t}{2}m_i^j D_\alpha u_i^j+\Delta t\, r_i, \tag{76}$$

where $m(x, t) = \Gamma(3 - \alpha)x^{2+\alpha}t$ and $r(x) = x^2$.

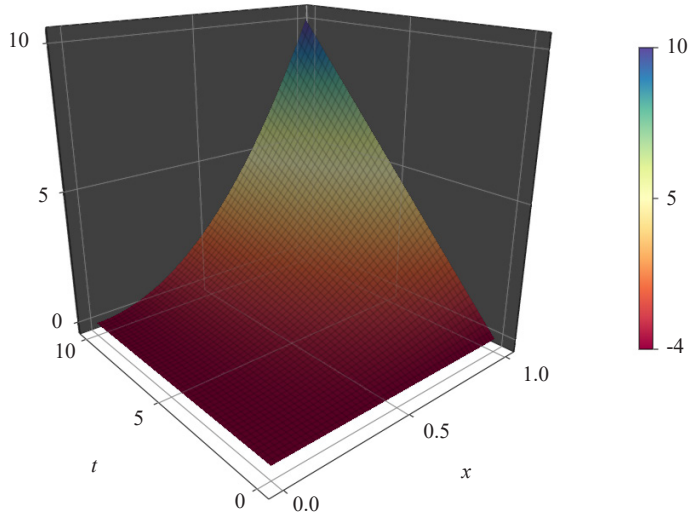

Figure 7. 3D plot of solution at $N = Nt = 50$, $\alpha = 1.5$

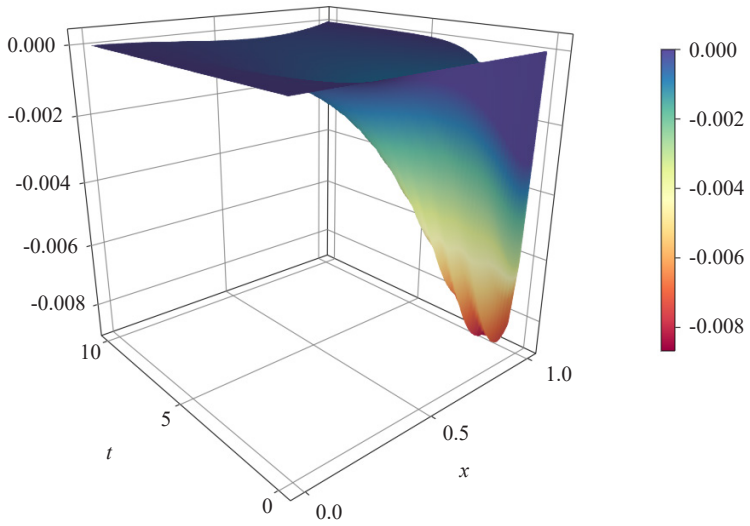

Figure 8. Error plot at $N = Nt = 50$, $\alpha = 1.5$

Table 13. Table of absolute errors at for different values of α when $N = Nt = 50$

x	$\alpha = 1.1$	$\alpha = 1.3$	$\alpha = 1.5$	$\alpha = 1.8$
0.10	7.540×10^{-6}	6.440×10^{-6}	5.810×10^{-6}	4.920×10^{-6}
0.30	4.020×10^{-5}	3.630×10^{-5}	3.230×10^{-5}	2.650×10^{-5}
0.50	8.730×10^{-5}	7.430×10^{-5}	6.300×10^{-5}	4.880×10^{-5}
0.70	1.120×10^{-4}	9.040×10^{-5}	7.380×10^{-5}	5.480×10^{-5}
0.90	6.670×10^{-5}	5.140×10^{-5}	4.060×10^{-5}	2.910×10^{-5}
0.98	1.630×10^{-5}	1.240×10^{-5}	9.640×10^{-6}	6.830×10^{-6}

Table 14. Convergence rates for different values of α when $N = Nt = 50$

x	$\alpha = 1.1$	$\alpha = 1.3$	$\alpha = 1.5$	$\alpha = 1.8$
0.10	2.0060	2.0247	2.0043	1.9986
0.30	1.9991	1.9991	1.9989	1.9989
0.50	2.0002	1.9993	1.9992	1.9991
0.70	1.9978	1.9991	1.9992	1.9994
0.90	1.9972	2.0002	1.9981	2.0017
0.98	1.9973	2.0017	2.0018	1.9976
Ord_∞	1.2139	1.4982	1.4987	1.4945

The approximate solution in Figure 7 is closest to the exact that in the first half of x interval and Figure 8 shows that the error propagates towards the end of the x-interval. The absolute errors in Table 13 decreases as α increases. Table 14 shows that for all $1 < \alpha < 2$, convergence order is approximately 2.

7. Conclusion

In conclusion, the OCFE method using quadratic B-Spline basis functions is computational efficient for solving the fractional space diffusion equation. The method is unconditionally stable and is convergent of order $(3 - \alpha)$, $1 < \alpha < 2$ for some of the examples. Various numerical simulations are presented in order to validate the robustness of the method. To the best of knowledge, this is the first time quadratic B-splines have been applied in the context of the OCFE method for solving the space fractional diffusion equation.

Acknowledgements

The authors are grateful for the conference funding received from the college of agriculture, engineering and

science (AES), university of KwaZulu-Natal, South Africa.

Conflict of interest

The authors declare no competing financial interest.

References

[1] Liu J, Fu H, Chai X, Sun Y, Guo H. Stability and convergence analysis of the quadratic spline collocation method for time-dependent fractional diffusion equations. *Applied Mathematics and Computation*. 2019; 346: 633-648. Available from: https://doi.org/10.1016/j.amc.2018.10.046.

[2] Meerschaert MM, Tadjeran C. Finite difference approximations for fractional advection-dispersion flow equations. *Journal of Computational and Applied Mathematics*. 2004; 172(1): 65-77. Available from: https://doi.org/10.1016/j.cam.2004.01.033.

[3] Tian W, Zhou H, Deng W. A class of second order difference approximations for solving space fractional diffusion equations. *Mathematics of Computation*. 2015; 84(294): 1703-1727. Available from: https://doi.org/10.1090/S0025-5718-2015-02917-2.

[4] Jin B, Lazarov R, Liu Y, Zhou Z. The Galerkin finite element method for a multi-term time-fractional diffusion equation. *Journal of Computational Physics*. 2015; 281: 825-843. Available from: https://doi.org/10.1016/j.jcp.2014.10.051.

[5] Mao Z, Shen J. Efficient spectral-Galerkin methods for fractional partial differential equations with variable coefficients. *Journal of Computational Physics*. 2016; 307: 243-261. Available from: https://doi.org/10.1016/j.jcp.2015.11.047.

[6] Sayevand K, Arjang F. Finite volume element method and its stability analysis for analyzing the behavior of sub-diffusion problems. *Applied Mathematics and Computation*. 2016; 290: 224-239. Available from: https://doi.org/10.1016/j.amc.2016.06.008.

[7] Salehi Y, Darvishi MT, Schiesser WE. Numerical solution of space fractional diffusion equation by the method of lines and splines. *Applied Mathematics and Computation*. 2018; 336: 465-480. Available from: https://doi.org/10.1016/j.amc.2018.04.053.

[8] Singh S, Singh S, Aggarwal A. A new spline technique for the time fractional diffusion-wave equation. *MethodsX*. 2023; 10: 102007. Available from: https://doi.org/10.1016/j.mex.2023.102007.

[9] Sayevand K, Yazdani A, Arjang F. Cubic B-spline collocation method and its application for anomalous fractional diffusion equations in transport dynamic systems. *Journal of Vibration and Control*. 2016; 22(9): 2173-2186. Available from: https://doi.org/10.1177/1077546316636282.

[10] Kolk M, Pedas A, Tamme E. Modified spline collocation for linear fractional differential equations. *Journal of Computational and Applied Mathematics*. 2015; 283: 28-40. Available from: https://doi.org/10.1016/j.cam.2015.01.021.

[11] Seidzadeh MS, Roohani GH, Etesami SK. An anomalous diffusion approach for speckle noise reduction in medical ultrasound images. *Computational Methods for Differential Equations*. 2022; 10(1): 225-235. Available from: https://doi.org/10.22034/cmde.2020.41858.1812.

[12] Ghehsareh HR, Raei M, Zaghian A. Application of meshless local Petrov-Galerkin technique to simulate two-dimensional time-fractional Tricomi-type problem. *Journal of the Brazilian Society of Mechanical Sciences and Engineering*. 2019; 41(6): 252. Available from: https://doi.org/10.1007/s40430-019-1749-0.

[13] Ghehsareh HR, Raei M, Zaghian A. Numerical simulation of a modified anomalous diffusion process with nonlinear source term by a local weak form meshless method. *Engineering Analysis with Boundary Elements*. 2019; 98: 64-76. Available from: https://doi.org/10.1016/j.enganabound.2018.10.004.

[14] Ghehsareh HR, Zaghian A, Zabetzadeh SM. An efficient meshless computational technique to simulate nonlinear anomalous reaction-diffusion process in two-dimensional space. *Nonlinear Dynamics*. 2019; 96(2): 1191-1211. Available from: https://doi.org/10.1007/s11071-019-04848-3.

[15] Raei M, Ghehsareh HR, Galletti A. An adaptive sparse kernel technique in greedy algorithm framework to simulate an anomalous solute transport model. *Engineering Analysis with Boundary Elements*. 2020; 121: 243-254. Available from: https://doi.org/10.1016/j.enganabound.2020.10.003.

[16] Ghehsareh HR, Zaghian A, Majlesi A. The method of approximate particular solutions to simulate an anomalous mobile-immobile transport process. *Mathematical Methods in the Applied Sciences*. 2020; 43(6): 3637-3649. Available from: https://doi.org/10.1002/mma.6144.
[17] Saadatmandi A, Dehghan M. A tau approach for solution of the space fractional diffusion equation. *Computers & Mathematics with Applications*. 2011; 62(3): 1135-1142. Available from: https://doi.org/10.1016/j.camwa.2011.04.014.
[18] Sousa E. Numerical approximations for fractional diffusion equations via splines. *Computers & Mathematics with Applications*. 2011; 62(3): 938-944. Available from: https://doi.org/10.1016/j.camwa.2011.04.015.